

Supporting Information

**Rational Design of ER α Targeting Hypoxia Turn-on Fluorescent
Probes with Antiproliferative Activity for Breast Cancer**

Qiuyu Meng,^{‡a} Baohua Xie,^{‡a} Xiaoyu Ma,^a Zhiye Hu,^a Fuling Zhou,^b Hai-Bing Zhou,^{a,c} * Chune Dong^{a*}

^a Hubei Province Engineering and Technology Research Center for Fluorinated Pharmaceuticals, State Key Laboratory of Virology, Wuhan University School of Pharmaceutical Sciences, Wuhan 430071, China. Email: cdong@whu.edu.cn, zhouhb@whu.edu.cn. Tel: 862768759586.

^b Department of Hematology, Zhongnan Hospital, Wuhan University, Wuhan 430071, China.

^c Medical Research Institute, Frontier Science Center for Immunology and Metabolism, Wuhan University, Wuhan 430071, China;

[‡] These two authors contributed equally to this work.

Table of contents

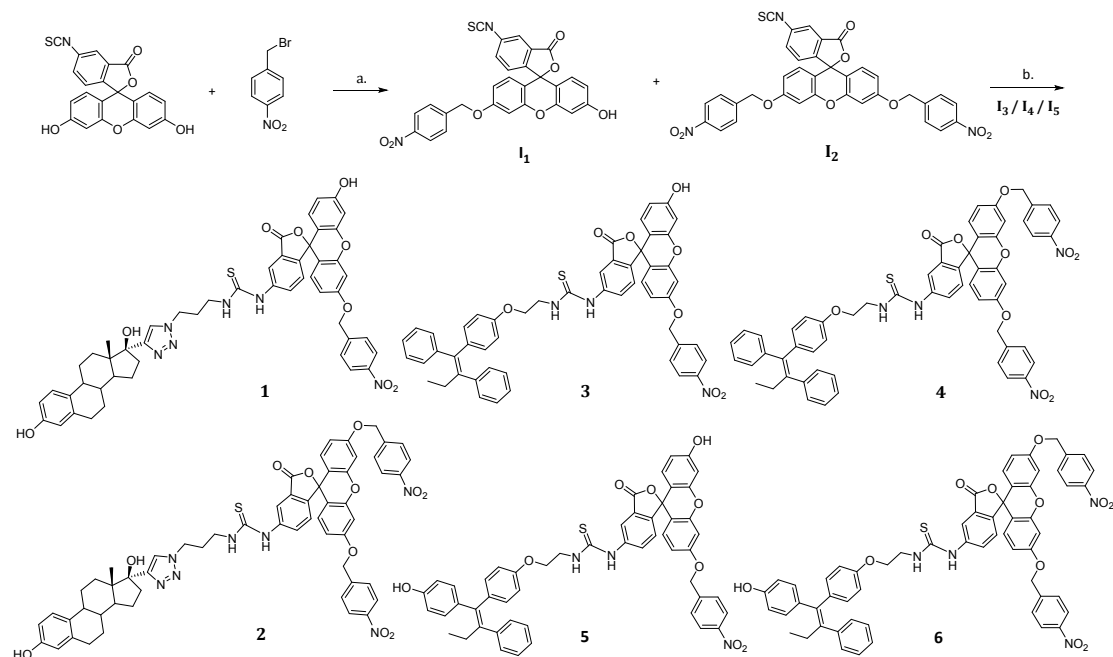
1. MATERIALS AND INSTRUMENTS.....	S2
2. SYNTHESIS OF PROBES 1-6.....	S2
3. HPLC ANALYST OF CELL CULTURE SOLUTION.....	S7
4. OPTICAL PROPERTIES.....	S7
5. ESTROGEN RECEPTOR BINDING AFFINITY	S7
6. LIVING CELLS IMAGING.....	S7
7. SELECTIVITY.....	S8
8. CELL VIABILITY ASSAY.....	S8
9. COMPARISON OF PROBE 5 WITH HYPOXIA FLUORESCENT PROBES.....	S8
10. THE SIGNIFICANCE OF LIVE CELL STUDY USING THERANOSTIC PROBES.	S10
11. HPLC SPETRA OF CELL CULTURE SOLUTION INCUBATED WITH PROBE 3	S12
12. FLUORESCENT QUANTUM YIELD (Q _{FL}) OF PROBES 1-6.....	S13
13. RELATIVE BINDING AFFINITY (RBA) OF PROBES 1-6 TO ER β	S13
14. MOLECULAR MODELLING STUDY.	S13
15. SUBCELLULAR LOCALIZATION OF THE PROBES	S15
16. CO-STAINING OF ERA ANTIBODY AND PROBES 3 AND 5.....	S17
17. RESPONSE OF PROBES 3 AND 5 TO FORMYLHYDRAZINE.	S17
18. SELECTIVITY OF PROBE 5.....	S18
19. ¹ H NMR AND ¹³ C SPECTRA.....	S19
20. REFERENCES.	S25

1. Materials and instruments.

All the starting materials were purchased commercially and used directly without further purification. ^1H NMR and ^{13}C NMR spectra were measured on a Bruker Biospin AV400 (400 MHz) instrument. Chemical shifts were reported in ppm (parts per million) and were referenced to tetramethylsilane. Melting points were measured on the X-4 Beijing Tech melting point apparatus, the data were not corrected. UV spectra and fluorescence spectra were recorded with SHIMADZU UV-2600 and HITACHI F-4600, respectively. Cell imaging was observed with Leica-LCS-SP8 confocal laser scanning microscope.

2. Synthesis of probes 1-6.

Synthetic procedure of probes 1-6.



Scheme S1. Synthetic procedure of probes 1-6. Reagents and conditions: (a) K₂CO₃, DMF, rt, 12 h; (b) Et₃N, 40 °C, 44 h.

General synthetic procedure of intermediate I₁ and I₂.

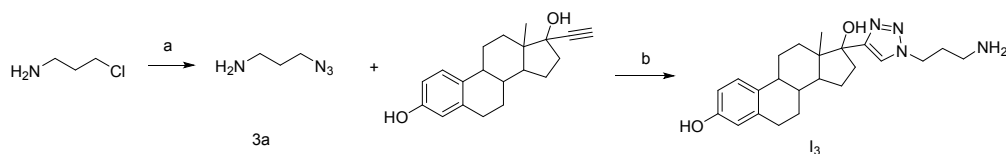
DMF (2 mL) was added to a mixture of K₂CO₃ (276 mg, 1.98 mmol) and FITC (130 mg, 0.33 mmol) under argon at 0 °C for 15 min, followed by the addition of 1-(bromomethyl)-4-nitrobenzene (72 mg, 0.33 mmol), stirred at room temperature in the dark for 12h. The residue was dissolved in saturated ammonium chloride aqueous solution (20 mL) and extracted with ethyl acetate (25 mL × 3). The organic layers were combined, dried over Na₂SO₄, concentrated *in vacuo*, and further purified by silica gel column chromatography (methanol/dichloromethane = 1:40) to provide I₁ as a yellow solid (61 mg, 35%). I₂ as a yellow solid was produced by the same procedure with 2 equivalents of 1-(bromomethyl)-4-nitrobenzene (85 mg, 42%).

I₁. Yield: 61 mg (35%), yellow solid. ^1H NMR (400 MHz, Acetone) δ 8.22 (d, J = 8.0 Hz, 2H), 7.99 (d, J = 7.1 Hz, 1H), 7.79-7.62 (m, 4H), 7.16 (d, J = 7.0 Hz, 1H), 6.90 (s, 1H), 6.73 (d, J = 8.7 Hz, 1H), 6.65 (d, J = 7.9 Hz, 2H), 6.54 (q, J = 8.7 Hz, 2H), 5.23 (s, 2H). ^{13}C NMR (101 MHz, DMSO-*d*₆) δ 165.27, 150.40, 147.51, 142.87, 134.12, 133.71, 131.35, 131.12, 130.45, 130.24, 129.92, 129.23, 123.79, 115.05, 103.65, 65.96, 55.34.

I₂. Yield: 85 mg (42%), yellow solid. ^1H NMR (400 MHz, DMSO-*d*₆) δ 8.35-8.23 (m, 3H), 8.03 (d, J = 8.6 Hz, 2H), 7.82 (m, 4H), 7.49 (d, J = 7.5 Hz, 1H), 7.28 (d, J = 8.6 Hz, 2H), 7.17 (d, J = 2.1 Hz, 1H), 6.96 (dd, J = 8.9, 2.2 Hz, 1H), 6.81 (dd, J = 14.8, 5.3 Hz, 2H), 6.37 (m, 1H), 6.09 (d, J = 1.7 Hz, 1H), 5.43 (s, 2H), 5.13 (s, 2H). ^{13}C NMR (101 MHz,

DMSO- d_6) δ 184.28, 165.22, 162.77, 158.49, 153.68, 149.67, 147.67, 147.56, 144.32, 142.87, 133.96, 131.44, 131.17, 130.75, 130.60, 130.00, 129.35, 128.86, 124.20, 123.83, 117.45, 115.05, 114.56, 105.02, 101.80, 69.36, 66.00, 55.38.

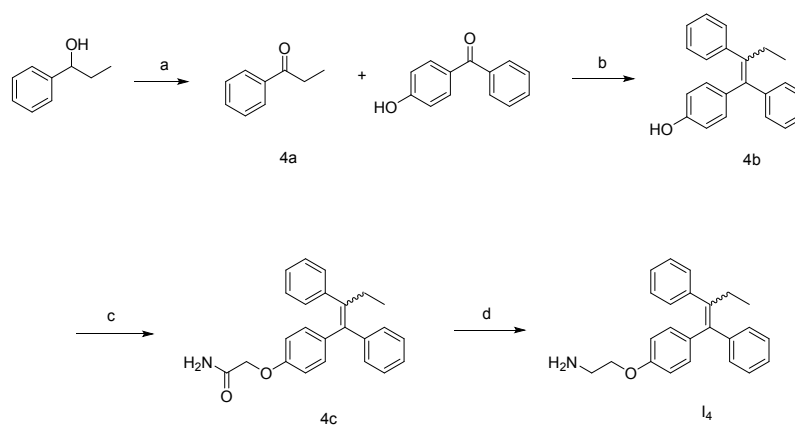
Synthetic procedure of intermediate **I**₃¹.



Scheme S1. Synthesis of intermediate **I**₃. Reagents and conditions: (a) NaN₃, H₂O, 80 °C, 12 h; (b) ascorbic acid, CuSO₄·5H₂O, *t*-BuOH/H₂O, 25 °C, 12 h.

NaN₃ (0.9 g, 13.8 mmol) was mixed into a solution of 3-chloropropylamine hydrochloride (0.6 g, 4.6 mmol) in H₂O (15 mL). This solution was heated to 80 °C for 12 h, cooled down, basified by KOH (1 mol/L) to pH = 9. The residue was dissolved in saturated ammonium chloride aqueous solution (20 mL) and extracted with ethyl acetate (30 mL × 3). The organic layers were combined and dried over Na₂SO₄, concentrated *in vacuo* to obtain **3a** as white oil. **3a** was used without further purification. A mixture of **3a** (100 mg, 1 mmol) and ethynyl estradiol (300 mg, 1 mmol) in *t*-BuOH (5 mL) was supplemented in H₂O (5 mL), ascorbic acid (20 mg, 0.11 mmol) and CuSO₄·5H₂O (30 mg, 0.12 mmol) were added, the mixture was stirred at 25 °C for 12 h. The crude mixture was diluted using ethyl acetate (40 mL) and 4:1 saturated NH₄Cl/NH₄OH (40 mL). The organic layer was separated and washed with 4:1 saturated NH₄Cl/NH₄OH (3 × 40 mL), dried, and concentrated *in vacuo* to yield **I**₃ (240 mg, 61.7%) as a white solid. ¹H NMR (400 MHz, CD₃OD): δ 7.84 (s, 1H), 6.98 (d, *J* = 8.4 Hz, 1H), 6.50 (d, *J* = 8.4 Hz, 1H), 6.47 (s, 1H), 4.44-4.49 (m, 2H), 2.71-2.78 (m, 3H), 2.43-2.50 (m, 1H), 2.07-2.12 (m, 4H), 1.80-2.00 (m, 4H), 1.51-1.64 (m, 3H), 1.35-1.43 (m, 2H), 1.24-1.32 (m, 1H), 1.04 (s, 3H), 0.65-0.70 (m, 1H).

Synthetic procedure of intermediate **I**₄.



Scheme S2. Synthesis of intermediate **I**₄. Reagents and conditions: (a) TCICA, pyridine, EtOAc, 95%; (b) Zn, TiCl₄, THF, 60%; (c) ICH₂CONH₂, acetone, K₂CO₃, 50%; (d) LAH, AlCl₃, THF, 75%.

Propiophenone (**4a**).

TCICA (1 g, 4.30 mmol) in ethyl acetate (10 mL) was added to the mixture of 1-phenylpropan-1-ol (1.36 g, 10 mmol), pyridine (0.95 g, 12 mmol) in ethyl acetate (10 mL) carefully and stirred for 5 min at rt. The mixture was filtered, and the filtrate was collected and washed with 1 M HCl (10 mL) and 5% NaHCO₃ respectively, extracted

with ethyl acetate (30 mL × 3). The organic layers were combined and dried over Na₂SO₄, concentrated *in vacuo* to obtain **4a** as transparent oil (1.27 g, 95%).

4-(1,2-Diphenylbut-1-en-1-yl)phenol (4b).²

Zinc powder (1.30 g, 20 mmol) was suspended in dry THF (20 mL), and the mixture was cooled to 0 °C. TiCl₄ (1.2 mL, 10 mmol) was added dropwise under argon. When the addition was complete, the mixture was warmed to room temperature and heated to reflux for 2 h. After cooling down, a solution of 4-hydroxybenzophenone (0.50 g, 2.53 mmol) and **4a** (1.10 g, 8.18 mmol) in dry THF (10 mL) was added at 0 °C and the mixture was heated at reflux in the dark for 2.5 h. After being cooled to room temperature, the zinc dust was filtered off and THF was evaporated. The residue was dissolved with saturated ammonium chloride aqueous solution (50 mL) and extracted with ethyl acetate (50 mL × 6). The organic layers were combined and dried over Na₂SO₄, concentrated *in vacuo*, and further purified by silica gel column chromatography (hexane/ethyl acetate = 30:1) to provide **4b** as a faint yellow solid (0.45 g, 60%).

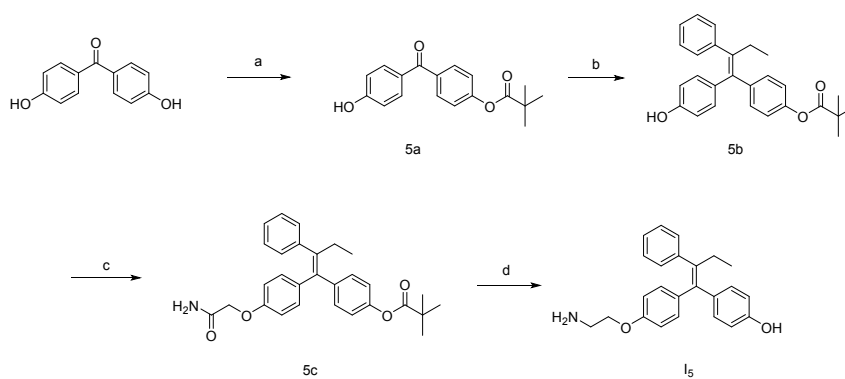
(E,Z)-2-(4-(1,2-diphenylbut-1-en-1-yl)phenoxy)acetamide (4c).

A suspension of **4b** (0.84 g, 2.8 mmol) and K₂CO₃ (2.18 g, 15.75 mmol) in acetone (20 mL) was heated to reflux for 10 min. A solution of 2-iodoacetamide (2.08 g, 11.25 mmol) in acetone (20 mL) was added, and the mixture was stirred for 3 h. After cooling down, acetone was evaporated and the residue was dissolved in saturated ammonium chloride aqueous solution (50 mL) and extracted with ethyl acetate (50 mL × 5). The organic layers were combined, dried over Na₂SO₄, concentrated *in vacuo*, and further purified by silica gel column chromatography (hexane/ethyl acetate = 4:1) to provide the **4c** as a faint yellow solid (0.50 g, 50%) of a 1:1 mixture of *E* and *Z* isomers.

(E,Z)-2-(4-(1,2-phenylbut-1-en-1-yl)phenoxy)ethan-1-amine (I₄).

A suspension of AlCl₃ (0.84 g, 6.32 mmol) and LiAlH₄ (1.22 g, 32.17 mmol) in dry THF (20 mL) was stirred under argon and cooled to 0 °C. A solution of **4c** (0.47 g, 1.30 mmol) in dry THF (10 mL) was added. The mixture was warmed to room temperature and stirred under argon for 3h. The reaction was quenched with H₂O (8 mL), and THF was evaporated. The residue was dissolved in saturated ammonium chloride aqueous solution (20 mL) and extracted with ethyl acetate (25 mL × 4). The organic layers were combined, dried over Na₂SO₄, concentrated *in vacuo*, and further purified by silica gel column chromatography (methanol/dichloromethane = 1:15) to provide the I₄ as a white solid (0.33 g, 75%) consisting of a 1:1 mixture of *E* and *Z* isomers. ¹H NMR (400 MHz, CDCl₃) δ 7.44-7.35 (m, 1H), 7.30 (t, *J* = 7.2 Hz, 1H), 7.26-7.11 (m, 6H), 7.03 (t, *J* = 6.8 Hz, 2H), 6.93 (d, *J* = 7.7 Hz, 2H), 6.83 (d, *J* = 8.4 Hz, 1H), 6.59 (d, *J* = 8.4 Hz, 1H), 4.05 (t, *J* = 4.7 Hz, 1H), 3.88 (t, *J* = 4.7 Hz, 1H), 3.13 (s, 1H), 3.03 (s, 1H), 2.54 (q, *J* = 12.3 Hz, 2H), 1.08-0.90 (t, *J* = 7.2 Hz, 3H). ¹³C NMR (101 MHz, CDCl₃) δ 157.52, 156.68, 143.80, 143.33, 142.37, 141.99, 141.44, 138.35, 136.32, 135.79, 131.96, 130.82, 130.67, 129.72, 129.48, 128.14, 127.91, 127.80, 127.33, 126.57, 126.07, 125.69, 114.10, 113.35, 69.47, 41.31, 29.04, 13.63.

Synthetic procedure of intermediate I₅.



Scheme S3. Synthesis of intermediate **I₅**. Reagents and conditions: (a) NaH, *t*-BuCOCl, THF, 51%; (b) propiophenone, Zn, TiCl₄, THF, 59%; (c) ICH₂CONH₂, acetone, K₂CO₃, 57%; (d) LAH, AlCl₃, THF, 70%.

4-Hydroxy-4'-(trimethylacetoxyl)benzophenone (**5a**).

Sodium hydride in 60% dispersion in mineral oil (0.44 g, 18.52 mmol) was added to a solution of 4,4'-dihydroxybenzophenone (2.14 g, 10 mmol) in dry THF (20 mL) under argon. The solution was stirred at rt for 30 min, cooled to 0 °C, treated with trimethylacetyl chloride (1.32 g, 10.95 mmol) and stirred for 1h after removing the ice-water bath. The reaction mixture was quenched with distilled water (10 mL) and extracted with ethyl acetate (50 mL × 3). The combined organic phase was dried and concentrated and further purified by silica gel column chromatography (dichloromethane/ethyl acetate = 70:1) to produce **5a** as a white solid. (1.52 g, 51%)

(*E*)-4-(1-(4-Hydroxyphenyl)-2-phenylbut-1-enyl)phenyl Pivalate (**5b**).³

5b was synthesized similar to the procedure of **4b**. The crude **5b** was provided by silica gel column chromatography (hexanes/ethyl acetate = 25:1) as a faint yellow solid (425 mg, 74%). Further rituration with methanol (2 mL) provided **5b** as the pure *E* isomer (*E*:*Z* > 100:1), a white solid (339 mg, 59%).

(*E*)-4-(1-(4-(2-Amino-2-oxoethoxy)phenyl)-2-phenylbut-1-enyl)-phenyl Pivalate (**5c**).

5c was synthesized similar to the procedure of **4c**. The preliminary **5c** was obtained by silica gel column chromatography (hexanes/ethyl acetate = 4:1) as a faint yellow solid (203 mg, 78.5%). Trituration with methanol (3 mL) provided **5c** as the pure *E* isomer (*E*:*Z* > 25:1), a white solid (147 mg, 57%).

(*Z*)-4-(1-(4-(2-Aminoethoxy)phenyl)-2-phenylbut-1-enyl)phenol (**I₅**).

I₅ was synthesized similar to the procedure of **I₄**. Purification by silica gel column chromatography (methanol/dichloromethane = 1:70) to provide **I₅** as a white solid (100 mg, 70%). The NMR spectrum indicated an *E*:*Z* ratio of 1:4.4. ¹H NMR (400 MHz, MeOD) δ 7.13-7.05 (m, 7H), 7.03 (m, 1.58H, *E* isomer), 6.95 (d, *J* = 8.5 Hz, 0.47H, *E* isomer), 6.78 (dd, *J* = 8.4, 5.0 Hz, 4H), 6.66 (d, *J* = 8.5 Hz, 0.47H, *E* isomer), 6.58 (d, *J* = 8.6 Hz, 2H), 6.42 (d, *J* = 8.5 Hz, 0.45H, *E* isomer), 4.05 (t, *J* = 5.2 Hz, 0.47H, *E* isomer), 3.88 (t, *J* = 5.2 Hz, 2H), 3.04 (t, *J* = 4.7 Hz, 0.45H, *E* isomer), 2.94 (t, *J* = 4.5 Hz, 2H), 2.50 (q, *J* = 7.5 Hz, 2H), 0.92 (t, *J* = 7.4 Hz, 3.5H). ¹³C NMR (101 MHz, DMSO-*d*₆) δ 157.77, 156.92, 156.70, 155.82, 142.74, 140.36, 140.16, 138.40, 136.21, 135.96, 134.31, 134.02, 131.90, 131.86, 130.62, 130.58, 129.86, 128.35, 128.32, 126.41, 126.37, 115.46, 114.79, 114.56, 113.78, 70.9, 69.83, 41.22, 29.04, 13.85.

General synthetic procedure of probes 1-6.

Et₃N (3 mL) was added to the mixture of equivalent **I₁** and **I₃**, **I₁** and **I₄**, **I₁** and **I₅** respectively under argon and stirred in the dark at 40 °C for 44 h, followed by the purification of prepared thin layer chromatography

(methanol/dichloromethane = 1:20) to obtain probes **1**, **3**, and **5** as yellow solids, respectively. Et₃N (3 mL) was added to the mixture of equivalent I₂ and I₃, I₂ and I₄, I₂ and I₅ respectively and stirred in the dark at 40 °C for 44 h, followed by the purification of prepared thin layer chromatography (methanol/dichloromethane = 1:20) to obtain probes **2**, **4**, **6** respectively as yellow solids.

Compound 1. Yield: 56 mg (43%), yellow solid (mp 150-153 °C). ¹H NMR (400 MHz, DMSO-*d*₆) δ 10.10 (s, 1H), 9.12 (s, 1H), 7.68 (s, 1H), 7.01-6.85 (m, 3H), 6.70 (m, 1H), 6.61 (dd, *J* = 8.5, 2.3 Hz, 3H), 6.51-6.47 (m, 5H), 6.42 (dd, *J* = 8.7, 2.9 Hz, 4H), 5.07 (s, 2H), 4.07 (t, *J* = 7.0 Hz, 2H), 3.54 (t, *J* = 7.1 Hz, 2H), 2.84-2.74 (m, 2H), 2.68 (m, 2H), 2.40-2.22 (m, 2H), 2.20-2.08 (m, 1H), 2.05-1.83 (m, 3H), 1.77 (t, *J* = 8.1 Hz, 3H), 1.52-1.32 (m, 4H), 0.89 (s, 3H). ¹³C NMR (101 MHz, DMSO-*d*₆) δ 181.80, 168.31, 158.71, 155.30, 154.29, 152.47, 152.42, 149.76, 147.68, 141.61, 137.62, 135.29, 133.66, 131.70, 131.00, 130.00, 129.35, 129.28, 127.92, 126.50, 126.36, 124.17, 122.94, 119.33, 115.35, 113.13, 112.84, 112.68, 110.83, 106.05, 102.58, 85.36, 81.44, 63.59, 55.37, 47.94, 47.10, 46.12, 43.56, 37.70, 35.58, 33.01, 31.75, 30.85, 27.02, 23.99, 14.83. HRMS (ESI) calcd for C₅₁H₄₈N₆O₉S [M+H]⁺, 921.3276; found 921.3253.

Compound 2. Yield: 50 mg (32%), yellow solid (mp 117-120 °C). ¹H NMR (400 MHz, DMSO-*d*₆) δ 9.93 (s, 1H), 8.97 (s, 1H), 8.22 (dd, *J* = 8.9, 5.5 Hz, 2H), 7.71-7.64 (m, 3H), 6.99-6.94 (m, 1H), 6.89 (dd, *J* = 7.4, 5.7 Hz, 2H), 6.84 (m, 1H), 6.76 (d, *J* = 3.2 Hz, 1H), 6.71-6.62 (m, 2H), 6.60 (m, 1H), 6.55-6.51 (m, 1H), 6.49-6.40 (m, 4H), 6.38-6.33 (m, 2H), 5.26 (s, 2H), 5.14 (s, 2H), 4.31 (t, *J* = 5.8 Hz, 2H), 3.46 (t, *J* = 4.6 Hz, 2H), 2.99 (m, 2H), 2.84 (m, 2H), 2.27 (m, 2H), 1.97-1.93 (m, 2H), 1.88-1.85 (m, 2H), 1.75 (qq, *J* = 5.2, 2.1 Hz, 3H), 1.45-1.36 (m, 4H), 0.86 (s, 3H). ¹³C NMR (101 MHz, DMSO-*d*₆) δ 180.03, 169.58, 161.64, 158.82, 155.35, 154.46, 148.83, 147.06, 141.33, 137.60, 134.98, 133.26, 130.87, 129.70, 128.77, 128.35, 126.44, 124.20, 124.02, 123.88, 123.15, 115.35, 113.13, 108.36, 106.08, 101.85, 84.97, 81.54, 70.16, 55.33, 49.06, 47.99, 43.62, 37.57, 34.91, 30.37, 29.73, 29.04, 27.65, 24.01, 14.84. HRMS (ESI) calcd for C₅₈H₅₃N₇O₁₁S [M+H]⁺, 1056.3597; found 1056.3549.

Compound 3. Yield: 45 mg (42%), yellow solid (mp 127-129 °C). ¹H NMR (400 MHz, MeOD) δ 8.20 (d, *J* = 7.5 Hz, 2H), 7.85 (s, 1H), 7.66-7.64 (m, 3H), 7.34 (d, *J* = 6.4 Hz, 2H), 7.23-7.18 (m, 2H), 7.10-7.03 (m, 6H), 7.01 (d, *J* = 7.5 Hz, 2H), 6.93-6.86 (m, 3H), 6.86 (d, *J* = 5.5 Hz, 2H), 6.75-6.71 (m, 2H), 6.67-6.61 (m, 2H), 6.56 (d, *J* = 8.4 Hz, 2H), 4.64 (s, 2H), 4.26 (s, 1H), 4.10-4.08 (t, *J* = 8.0 Hz, 1H), 3.44-3.37 (t, *J* = 2.8 Hz, 1H), 3.32-3.23 (t, *J* = 3.6 Hz, 1H), 2.47 (q, *J* = 13.4 Hz, 2H), 0.96-0.87 (t, *J* = 10.8 Hz, 3H). ¹³C NMR (100 MHz, DMSO-*d*₆) δ 181.85, 167.73, 160.19, 156.97, 156.61, 156.10, 155.75, 155.39, 155.36, 155.26, 147.70, 145.51, 140.68, 140.61, 140.38, 138.23, 136.91, 136.69, 134.28, 134.00, 131.95, 131.91, 131.81, 130.69, 130.57, 130.50, 129.85, 129.64, 128.40, 128.33, 127.50, 126.46, 124.28, 124.02, 123.73, 115.47, 114.80, 114.78, 113.95, 113.18, 109.43, 102.74, 65.71, 64.45, 44.95, 29.04, 13.89. HRMS (ESI) calcd for C₅₂H₄₁N₃O₈S [M+H]⁺, 868.2687; found 868.2683.

Compound 4. Yield: 33 mg (30%), yellow solid (mp 100-102 °C). ¹H NMR (400 MHz, DMSO-*d*₆) δ 10.00 (d, *J* = 9.0 Hz, 1H), 8.26 (dd, *J* = 8.8, 2.2 Hz, 2H), 7.71 (d, *J* = 7.5 Hz, 2H), 7.31 (m, 2H), 7.21-7.11 (m, 4H), 7.07 (dd, *J* = 13.4, 6.3 Hz, 3H), 7.03-6.96 (m, 3H), 6.95 (s, 1H), 6.91 (dd, *J* = 3.4, 2.4 Hz, 1H), 6.82 (m, 2H), 6.71 (m, 2H), 6.66-6.56 (m, 5H), 6.51-6.42 (m, 2H), 6.26 (d, *J* = 8.7 Hz, 1H), 5.54 (s, 2H), 5.29 (s, 2H), 3.69-3.60 (m, 1H), 3.53-3.46 (m, 1H), 3.27-3.18 (m, 1H), 3.16-3.05 (m, 1H), 2.36 (q, *J* = 12.1 Hz, 2H), 0.86-0.83 (t, *J* = 9.0 Hz, 3H). ¹³C NMR (100 MHz, DMSO-*d*₆) δ 181.85, 174.78, 159.09, 156.99, 152.39, 149.94, 147.50, 145.10, 142.21, 141.73, 131.66, 130.66, 130.45, 129.79, 129.39, 128.71, 128.65, 128.37, 128.27, 127.87, 124.10, 114.29, 113.52, 113.06, 106.03, 83.26, 68.78, 67.75, 49.07, 29.50, 13.78. HRMS (ESI) calcd for C₅₉H₄₆N₄O₁₀S [M+H]⁺, 1003.3007; found 1003.2992.

Compound 5. Yield: 43 mg (45%), yellow solid (mp 133-136 °C). ¹H NMR (400 MHz, MeOD) δ 8.21 (d, *J* = 8.7 Hz, 2H), 7.86 (s, 1H), 7.63 (dd, *J* = 15.6, 9.3 Hz, 3H), 7.26-7.17 (m, 1H), 7.17-7.13 (m, 2H), 7.11 (m, 3H), 7.06 (m, 2H), 7.01 (m, 2H), 6.80 (dd, *J* = 11.7, 8.6 Hz, 2H), 6.70 (d, *J* = 2.0 Hz, 2H), 6.68-6.62 (m, 3H), 6.61 (s, 1H), 6.55 (dd, *J* = 8.6, 2.4 Hz, 2H), 6.42 (d, *J* = 8.5 Hz, 1H), 4.64 (s, 2H), 4.30-4.20 (t, *J* = 4.0 Hz, 1H), 4.12-4.06 (t, *J* = 2.4 Hz, 1H), 3.44-3.35 (t, *J* = 3.6 Hz, 1H), 3.32-3.25 (t, *J* = 2.6 Hz, 1H), 2.48 (q, *J* = 14.9 Hz, 2H), 0.91 (t, *J* = 6.4 Hz, 3H). ¹³C NMR (100 MHz,

MeOD) δ 174.73, 156.87, 156.00, 145.60, 145.07, 143.18, 142.27, 142.14, 142.00, 140.84, 138.39, 136.91, 131.65, 130.45, 130.39, 130.34, 129.91, 129.47, 129.44, 129.36, 129.17, 129.00, 127.87, 127.55, 127.49, 127.00, 125.84, 125.41, 123.74, 123.46, 123.41, 123.33, 114.03, 113.20, 102.18, 63.84, 43.88, 39.06, 28.38, 12.49. HRMS (ESI) calcd for $C_{52}H_{41}N_3O_9S$ $[M+H]^+$, 884.2636; found 884.2639.

Compound 6, Yield: 52 mg (33%), yellow solid (mp 112-114 °C). 1H NMR (400 MHz, DMSO- d_6) δ 9.95 (s, 1H), 9.20 (s, 1H), 8.26 (dd, J = 8.8, 2.5 Hz, 2H), 7.71 (d, J = 8.3 Hz, 2H), 7.16 (m, 3H), 7.11-7.02 (m, 4H), 7.00-6.92 (m, 3H), 6.90 (d, J = 2.0 Hz, 1H), 6.86 (d, J = 2.4 Hz, 1H), 6.74-6.67 (m, 3H), 6.66-6.62 (m, 2H), 6.61-6.55 (m, 4H), 6.54-6.53 (m, 1H), 6.50 (s, 1H), 6.45 (s, 1H), 6.38 (d, J = 8.5 Hz, 1H), 6.24 (d, J = 8.8 Hz, 1H), 5.52 (s, 2H), 5.29 (s, 2H), 3.69-3.66 (t, J = 12.0 Hz, 2H), 3.21 (t, J = 13.9 Hz, 2H), 2.36 (q, J = 13.4 Hz, 2H), 0.85-0.80 (t, J = 10.0 Hz, 3H). ^{13}C NMR (100 MHz, DMSO- d_6) δ 181.82, 174.93, 161.81, 156.58, 156.70, 149.93, 147.52, 145.08, 142.70, 140.48, 138.31, 131.92, 131.84, 130.64, 130.58, 129.85, 128.66, 128.31, 126.43, 125.05, 124.10, 115.54, 114.77, 113.79, 106.04, 85.46, 66.61, 66.39, 55.37, 27.06, 13.82. HRMS (ESI) calcd for $C_{59}H_{46}N_4O_{11}S$ $[M+H]^+$, 1019.2957; found 1019.2933.

3. HPLC analyst of cell culture solution.

The breast cancer cell line MCF-7 cells were cultured using Dulbecco's Modified Eagle Medium (DMEM) containing 10% fetal bovine serum (FBS) in an atmosphere of 5% CO₂ and 95% air at 37 °C. Before staining, the cells were plated in 35 mm glass-bottom culture dishes and allowed to adhere for 24 h. MCF-7 cells were washed with PBS and treated with probe **3** (10 μ M) under hypoxia condition produced by anaerobic bags at 37 °C for 12 h. The cell culture solution was then collected after the addition of 0.2% Triton X-100 for 10 min. Ethyl acetate was added to the solution followed by sonication and centrifugation. The organic layer was carefully collected and dried before HPLC analyst.

4. Optical properties.

Optical properties of the probes were examined in 10 mM PBS (pH = 7.4) solution using a Varian Cary 100 UV-vis spectrophotometer and Varian Cary Eclipse fluorescence spectrophotometer. For the determination of the fluorescent quantum yield, fluorescein in 10 mM PBS was used as a standard ($\Phi_f = 0.95$). Values were calculated according to the following equation.

$$\Phi_{\text{(sample)}} = \Phi_{\text{(standard)}} \times (A_{\text{(standard)}} / A_{\text{(sample)}}) \times (S_{\text{(sample)}} / S_{\text{(standard)}})$$

In which Φ represents fluorescent quantum yield, $A_{\text{(standard)}}$ and $A_{\text{(sample)}}$ represent the absorption of the standard and the sample at the excitation wavelength respectively, $S_{\text{(standard)}}$ and $S_{\text{(sample)}}$ represent the fluorescence emission peak of the standard and the sample respectively. Excitation: 497 nm, slit = 10/10 nm.

5. Estrogen receptor binding affinity.

Relative binding affinities (RBAs) were determined by a fluorescence polarization assay (FPA) as previously described.⁴ Briefly, 40 nM of a fluorescence tracer and 0.8 μ M purified human ER α or ER β ligand binding domains (LBD) were diluted in 100 mM potassium phosphate buffer (pH = 7.4) containing 100 μ g mL⁻¹ bovine gamma globulin (Sigma-Aldrich, MO). Incubation was carried out for 2 h at room temperature (25 °C) keeping in dark. Fluorescence polarization values were then measured using citation 3 microplate reader (Biotek). The binding affinities were expressed as relative binding affinity (RBA) values with the RBA of 17 β -estradiol set to be 100. The values given were the average \pm range of two independent determinations.

6. Living cells imaging.

The breast cancer cell line MCF-7 and MDA-MB-231 were cultured using Dulbecco's Modified Eagle Medium containing 10% fetal bovine serum in an atmosphere of 5% CO₂ and 95% air at 37 °C. Before the imaging

experiments, the cells were plated in 35 mm glass-bottom culture dishes and allowed to adhere for 24 h. Cells were washed with PBS buffer before the co-incubation with the probes. Hypoxia environment was produced by the use of anaerobic bags. Hypoxic images on MCF-7 cells and MDA-MB-231 cells were obtained upon the addition of probes **1-6** (10 μ M) to the culture medium under hypoxic environment at 37 °C overnight. Images on MCF-7 cells under normoxic condition were obtained upon the addition of probes **1-6** to the culture medium in an atmosphere of 5% CO₂ and 95% air at 37 °C overnight. In localization experiments, probes **1-6** were added to MCF-7 cells overnight under hypoxia condition followed by the addition of DAPI to stain nucleus.

For immunofluorescence co-staining, the cells were incubated with the probes **3** and **5** (10 μ M) under hypoxia condition at 37 °C for 12 h. Then the cells were fixed in 4% paraformaldehyde, permeabilized with 0.2% Triton X-100 for 10 min, washed 3 times with PBS and incubated 12 h at 37 °C with Monoclonal anti-ER α antibody (1:200, purchased from Sigma-Aldrich). After incubation, the culture dishes were washed with PBS and incubated with DyLight 594 AffiniPure Goat Anti-Rabbit IgG (1:200, purchased from Abbkine) for 1 h. After washing with PBS, the cells were incubated with DAPI for 10 min. The cells were observed with Leica-LCS-SP8 confocal laser scanning microscope. Excitation: 497 nm for **3** and **5**, 594 nm for ER α antibody, 405 nm for DAPI.

7. Selectivity.

Cellular interfering analytes including cation, anion, amino acids, various reactive oxygen species and other reductive substances were added to the PBS buffer solution (10 mM, pH = 7.4) of probe **5** (5 μ M) respectively. The control group was added formylhydrazine. Secondary water was added to reach 3 mL of the whole volume, and the fluorescent intensity was measured with HITACHI F-4600 (Slit = 10/10 nm). Fluorescent response of probe **5** (5 μ M) to various species: 1, blank; 2, NaCl (100 mM); 3, KCl (100 mM); 4, MgCl₂ (2.5 mM); 5, H₂O₂ (100 μ M); 6, Tyr (1 mM); 7, His (1 mM); 8, GSH (1 mM); 9, Gly (1 mM); 10, Glu (1 mM); 11, Cys (1 mM); 12, Ala (1 mM); 13, CO (100 μ M); 14, H₂S (100 μ M); 15, HClO (100 μ M); 16, ¹O₂ (100 μ M); 17, \cdot OH (100 μ M); 18, Formylhydrazine (100 μ M) was tested. Excitation: 497 nm, slit = 10/10 nm.

The substances were prepared as follow.

(1) CO: Carbon monoxide is produced by the carefully addition of formic acid into concentrated sulfuric acid heated at 80~90 °C. $\text{HCOOH} + \text{H}_2\text{SO}_4 = \text{CO} + \text{H}_2\text{O}$

(2) H₂S: Hydrogen sulfide was prepared by the reaction of ferrous sulfide and dilute sulfuric acid. The concentration of H₂S was equal to the ferrous sulfide. $\text{FeS} + \text{H}_2\text{SO}_4 = \text{FeSO}_4 + \text{H}_2\text{S}$

(3) \cdot OH: Hydroxyl radical was produced by Fenton reaction. To generate \cdot OH, ferrous chloride was added in the presence of 10 equiv of H₂O₂. The concentration of \cdot OH was equal to the Fe(II) concentration.

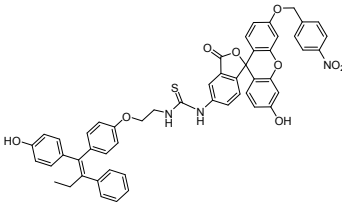
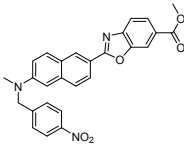
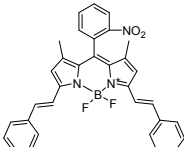
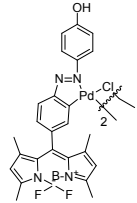
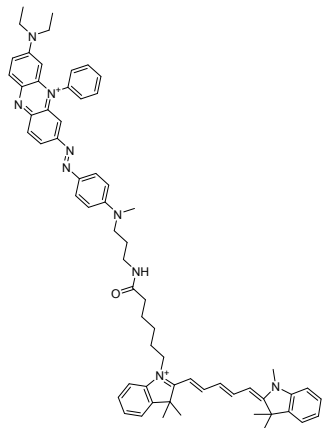
(4) ¹O₂: Singlet oxygen was produced by the reaction of H₂O₂ with ClO⁻. $\text{ClO}^- + \text{H}_2\text{O}_2 = \text{}^1\text{O}_2 + \text{H}_2\text{O} + \text{Cl}^-$

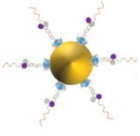
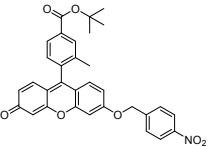
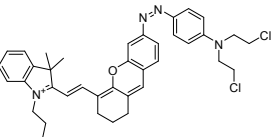
8. Cell viability assay.

The human breast cancer cell line MCF-7 and normal breast cells MCF-10A were obtained from ATCC. Cells were maintained in DMEM with 10% FBS. For all experiments, cells were grown in 96-well microtiter plates (Nest Biotech Co., China) with appropriate ligand triplicates for 72 h. MTT colorimetric tests (Biosharp, China) were employed to determine cell viability per the manufacturer's instructions. IC₅₀ values were calculated according to the following equation: $Y = 100\% \text{ inhibition} + (0\% \text{ inhibition} - 100\% \text{ inhibition}) / (1 + 10^{[(\text{Log}(C_{50} - X) \times \text{Hillslope})]})$, where Y = fluorescence value, and X = log_[inhibitor]. The experiments were repeated three times at least.

9. Comparison of probe **5** with hypoxia fluorescent probes.

Table S1 Comparison of probe **5** with some hypoxia fluorescent probes.

	Structure	λ_{ex} (nm)	λ_{em} (nm)	Application	Ref.
1	 <p style="text-align: center;">5</p>	497	523	ER α monitor and ER $^+$ Breast cancer detection and inhibition	The present work
2	 <p style="text-align: center;">Probe 1</p>	398	494	Nitroreductase detection, hypoxic status monitoring in tumor cells and tissues	<i>Anal. Chem.</i> , 2015, 87 , 11832-11839
3	 <p style="text-align: center;">BDP-NO₂</p>	649	670	Targeted detection of myocardial hypoxia in living cells and in vivo	<i>Anal. Chem.</i> , 2019, 91 , 6585-6592
4	 <p style="text-align: center;">ACP-1</p>	498	512	CO fluctuation tracking in the hypoxic cells	<i>Anal. Chem.</i> , 2016, 88 , 11154-11159
5	 <p style="text-align: center;">QCy5</p>	650	670	<i>In Vivo</i> real-time imaging of acute ischemia	<i>J. Am. Chem. Soc.</i> , 2010, 132 , 15846-15848

6	 <p>AuNPs</p>	561	580	Quantitative analysis and <i>in situ</i> imaging of cytochrome c under hypoxic condition	<i>Anal. Chem.</i> , 2018, 90 , 5865-5872
7	 <p>FBN-1</p>	490	515	Detection of hypoxic cancer cells	<i>ACS Sens.</i> , 2017, 2 , 1139-1145
8	 <p>Probe 1</p>	670	705	Tracking of hypoxia activated cancer chemotherapy <i>in vivo</i>	<i>Chem. Commun.</i> , 2019, 55 , 13172-13175

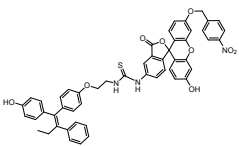
Common ground: (1) All hypoxia fluorescent probes contain hypoxia reductive group such as nitro or azo groups. (2) The hypoxia responsive group can quench fluorescence and display hypoxia turn-on property. (3) Many hypoxia turn-on probes can target the hypoxic environment of cancers, and some of them have shown the antiproliferative effects for cancer theranostics.

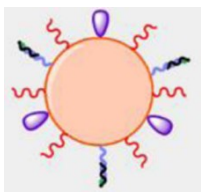
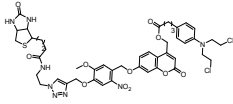
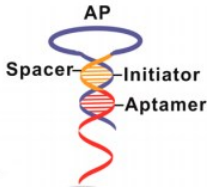
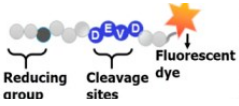
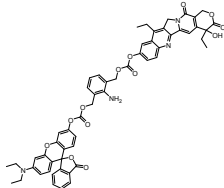
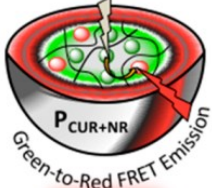
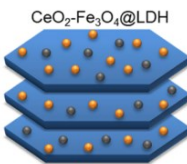
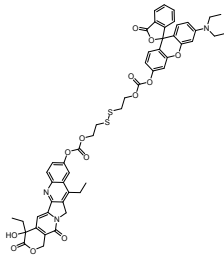
Differentia: (1) Different hypoxia probes conjugate different fluorophores, which leads to different maximum excitation wavelengths and maximum emission wavelengths, and thus be applied in live cell detection or *in vivo* imaging. (2) Different hypoxia probes have different applications, for examples, cancer cell imaging, cancer chemotherapy tracking, signal molecule detection (e.g. CO), bioprotein analyst (e.g. nitroreductase detection).

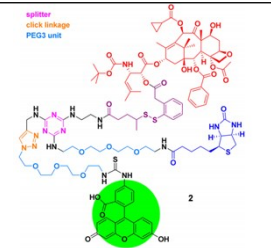
Many hypoxia probes are designed to target the tumor hypoxia microenvironment and can image certain cancer cell lines, but the selective detection for a specific cancer awaits improvement. In contrast, our probes were designed to target both the biomarker of ER α protein and the hypoxia environment of breast cancer cells, which can specifically image ER α protein and ER $^+$ breast cancer cells.

10. The significance of live cell study using theranostic probes.

Table S2 Theranostic probes for live cell study.

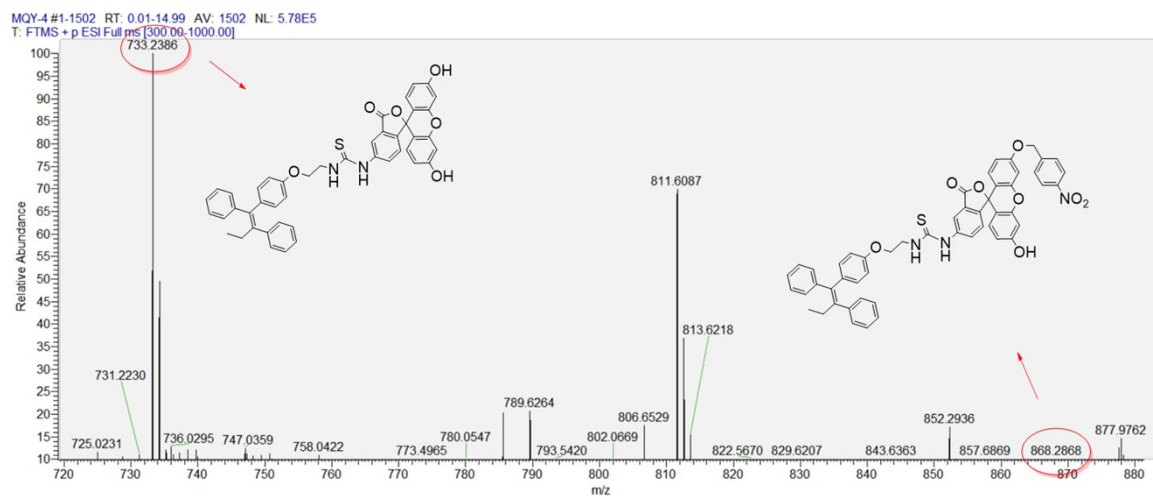
	Design	λ_{ex} (nm)	λ_{em} (nm)	Application	Ref.
1	 <p>5</p>	497	523	ER α monitor, ER $^+$ Breast cancer detection and inhibition	The present work

2		488	518	Cancer cells and miRNA-21 imaging, cancer cell inhibition	<i>Anal. Chem.</i> , 2014, 86 , 3602-3609
3		-	546	Drug delivery and monitor in cancer cells	<i>J. Mater. Chem. B</i> , 2015, 3 , 728-732
4		-	660	Cancer cell detection, anticancer drug delivery in cancer cells	<i>Anal. Chem.</i> , 2015, 87 , 6470-6474
5		550	580	Real-time imaging of caspase-induced cell apoptosis, <i>in situ</i> apoptosis induction	<i>Anal. Chem.</i> , 2016, 88 , 11184-11192
6		515	548	H ₂ S-based cancer cell monitor and inhibition	<i>ACS Appl. Bio Mater.</i> , 2019, 2 , 1322-1330
7		420	540 & 600	Live cell bioimaging, drug delivery in cancer cells	<i>ACS Appl. Bio Mater.</i> , 2019, 2 , 5245-5262
8		485	535	ROS scavenging and imaging in living cells	<i>ACS Appl. Bio Mater.</i> , 2019, 2 , 5930-5940
9		510	550	Cancer cell inhibition and drug delivery monitor	<i>ACS Appl. Mater. Interfaces</i> , 2016, 8 , 33430-33438

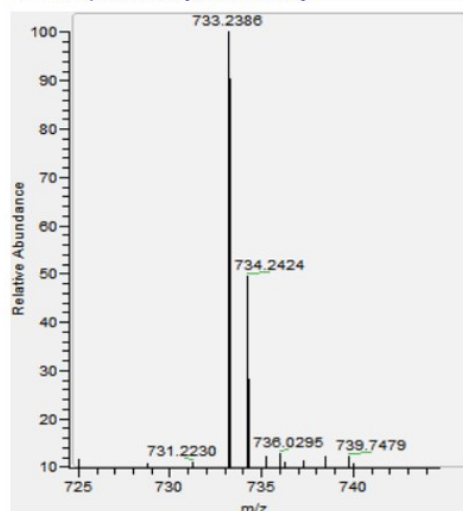
10		488	527	Cancer cell imaging and drug delivery in cancer cells	<i>J. Med. Chem.</i> , 2015, 58 , 2406-2416
----	---	-----	-----	---	--

In recent years, the use of theranostic probes for live cell study has attracted much attention, it can not only image the cellular level of important biomarkers or molecules, but also exert inhibitory effects on targeted cells, which benefits both the understand of biomarkers and drug development.

11. HPLC spectra of cell culture solution incubated with probe 3.

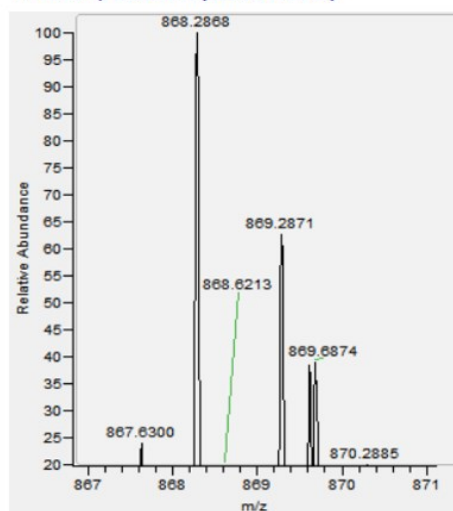


MQY-4 #1-1502 RT: 0.01-14.99 AV: 1502 NL: 5.78E5
T: FTMS + p ESI Full ms [300.00-1000.00]



$C_{45}H_{36}N_2O_6S [M+H]^+$
Calcd. : 733.2667
Found : 733.2386

MQY-4 #1-1502 RT: 0.01-14.99 AV: 1502 NL: 3.27E4
T: FTMS + p ESI Full ms [300.00-1000.00]



$C_{52}H_{41}N_3O_8S [M+H]^+$
Calcd. : 868.2687
Found : 733.2868

Fig. S1 HPLC spectra of cell culture solution incubated with probe 3. MCF-7 cells were treated with probe 3 (10 μ M) under hypoxia condition produced by anaerobic bags at 37 $^{\circ}$ C for 12 h, then the cell culture solution was collected and processed before HPLC analyst.

12. Fluorescent quantum yield (Q_{fl}) of probes 1-6.

Table S3 Fluorescent quantum yield of probes 1-6 in PBS solution (pH = 7.4)^a.

Compound	1	2	3	4	5	6
Φ_{fl}	0.041	0.038	0.053	0.042	0.049	0.044

^a Fluorescence quantum yields (Φ_{fl}) were determined using fluorescein ($\Phi_{fl} = 0.95$) as a reference.

13. Relative binding affinity (RBA) of probes 1-6 to ER β .

Table S4 Relative binding affinity (RBA) of probes 1-6 to ER β ^a.

Compound	RBA	Compound	RBA	Compound	RBA
1	< 0.01	3	0.77	5	0.59
2	< 0.01	4	0.06	6	< 0.01

^aRelative binding affinity (RBA) values are determined by competitive radiometric binding assays and are expressed as $IC_{estradiol} 50 / IC_{compound} 50 \times 100 \pm$ the range or standard deviation (RBA, estradiol = 100%).

14. Molecular modelling study.

Docking simulation was performed with ER α LBD crystal structure which was extracted from PDB: 1ERE and ER β LBD crystal structure extracted from PDB: 1YYE.⁵⁻⁶ Probes were docked into the three-dimensional structure of ER α LBD or ER β LBD using AutoDock software (version 4.2). A docking cube with edges of 60 Å, 60 Å, and 58 Å in the X, Y, and Z dimensions, respectively (a grid spacing of 0.375 Å), which existed in the entire active site, was used throughout docking process. Based on the Lamarckian genetic algorithm (LGA), 80 runs were performed for each ligand with 500 individuals in the population. The figures were prepared using PyMOL.

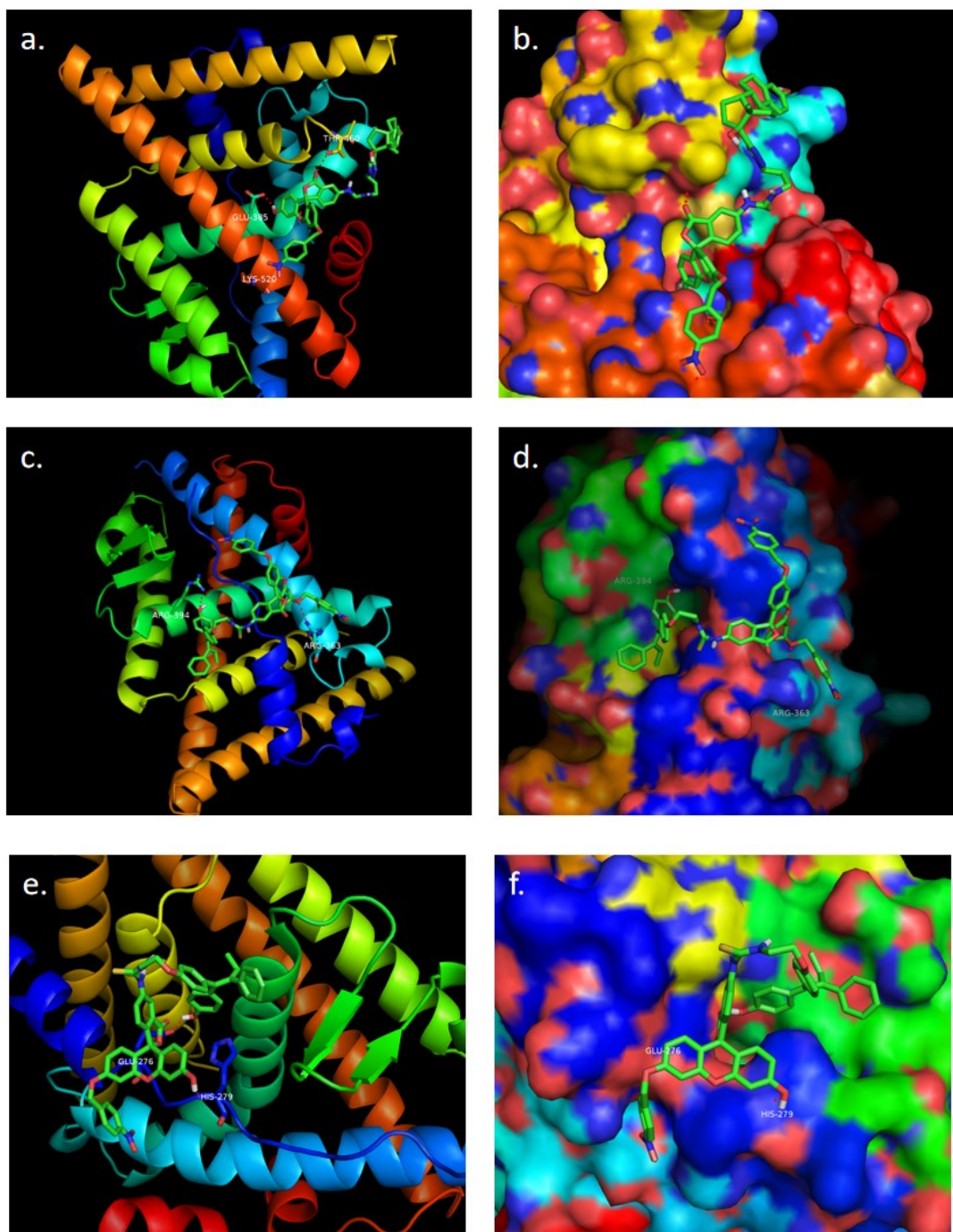
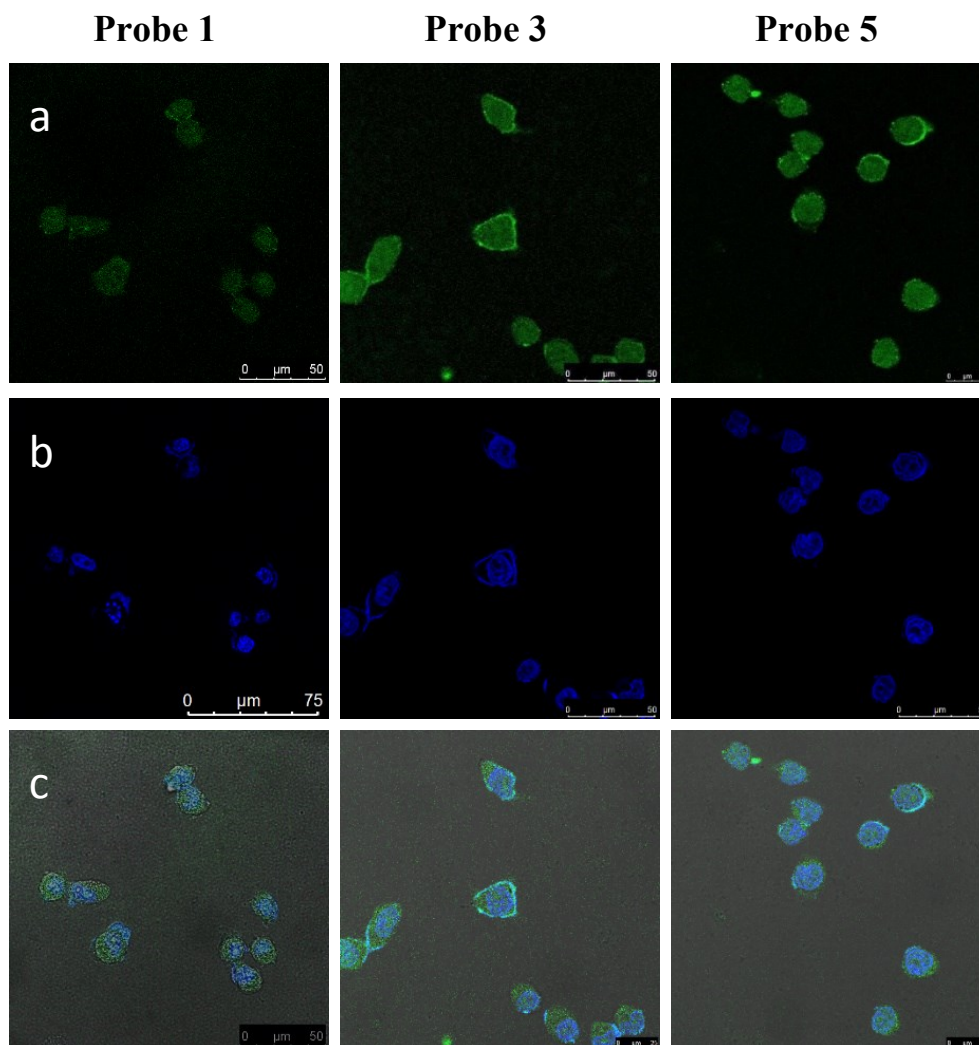


Fig. S2 Molecular modelling of probes 1 and 6 bound to ER α (1ERE) and probe 5 bound to ER β (1YYE). (a) Probe 1 bound to ER α LBD shown as helix; (b) Probe 1 bound to ER α LBD shown as solid; (c) Probe 6 bound to ER α LBD shown as helix; (d) Probe 6 bound to ER α LBD shown as solid. (e) Probe 5 bound to ER β LBD shown as helix; (f) Probe 5 bound to ER β LBD shown as solid.

15. Subcellular localization of the probes.



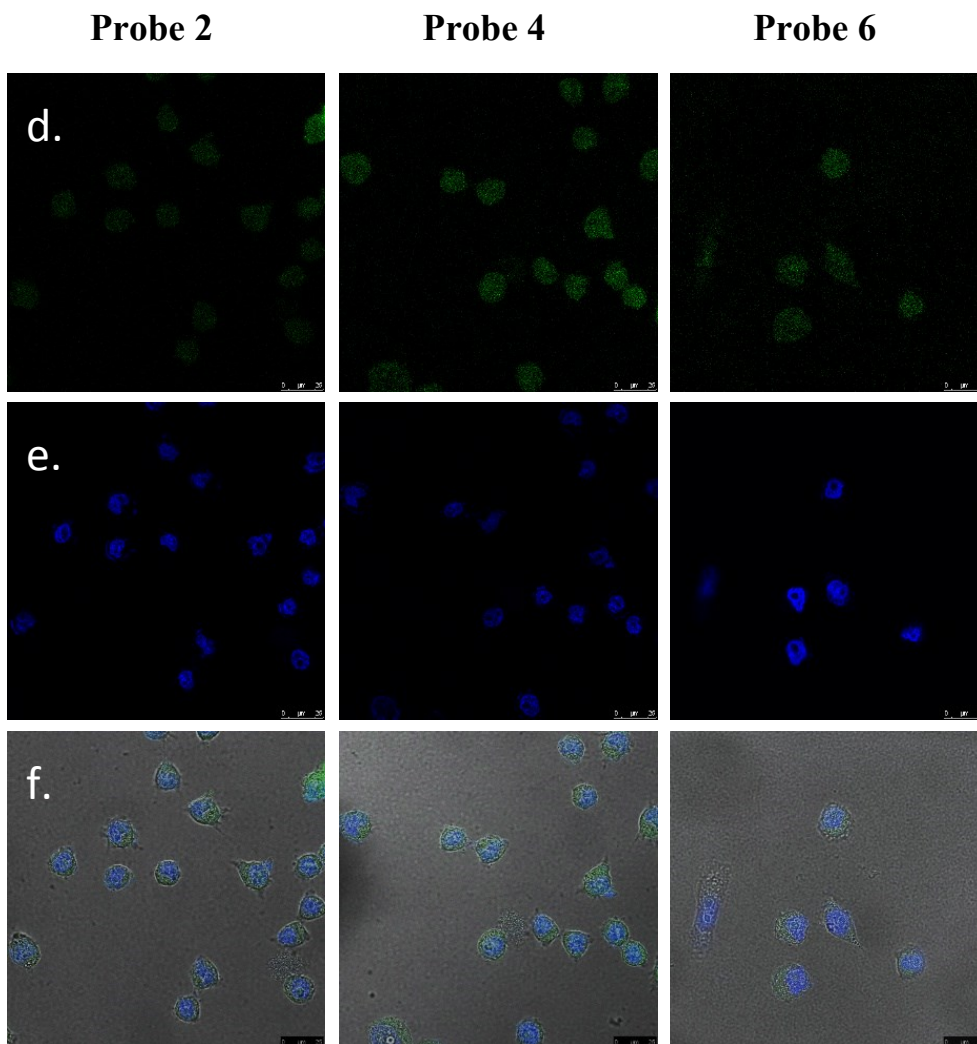


Fig. S3 Magnified images of MCF-7 cells incubated with probes **1-6** (10 μ M) under hypoxia condition. (a) (d) Images of MCF-7 cells treated with probes **1-6** respectively under hypoxia condition produced by anaerobic bags at 37 $^{\circ}$ C. (b) (e) Images of MCF-7 cells treated with probes **1-6** respectively under hypoxia condition followed by the addition of DAPI to stain the nuclei and collected in DAPI channel. (c) (f) Corresponding merged images of MCF-7 cells.

16. Co-staining of ER α antibody and probes 3 and 5.

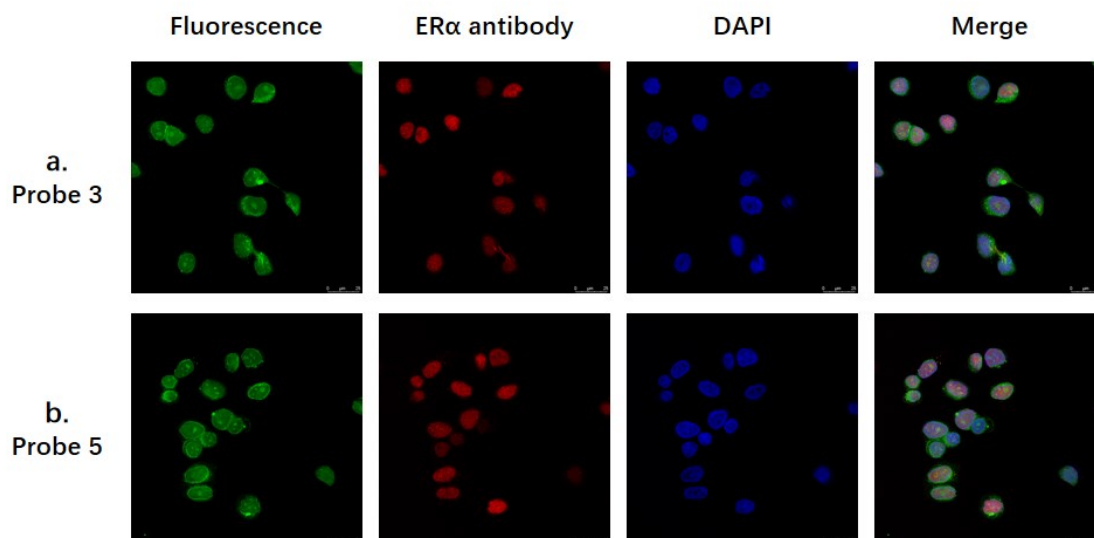


Fig. S4 Co-localization study of MCF-7 cells incubated with the probes, DAPI and ER α antibody under hypoxia condition. (a) Co-staining of MCF-7 cells with probe **3** (10 μ M), DAPI and ER α antibody. (b) Co-staining of MCF-7 cells with probe **5** (10 μ M), DAPI and ER α antibody.

17. Response of probes 3 and 5 to formylhydrazine.

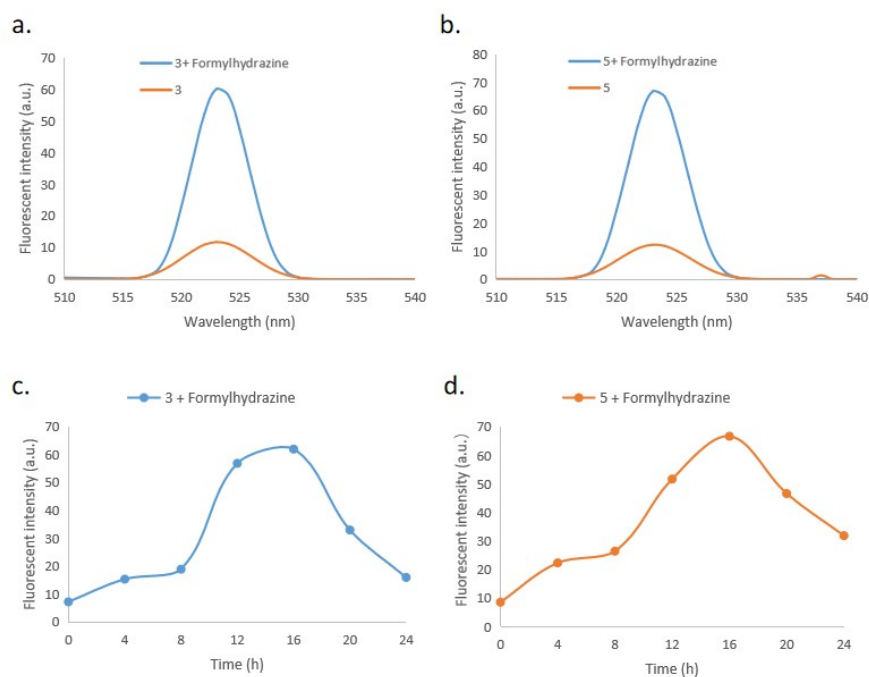


Fig. S5 Fluorescent response of probes **3** and **5** (1 μ M) to formylhydrazine. (a) Fluorescent response of **3** treated with formylhydrazine. (b) Fluorescent response of **5** treated with formylhydrazine. (c) Response of **3** treated with formylhydrazine after 0h, 4h, 8h, 12h, 16h, 20h and 24h. (d) Response of **5** treated with formylhydrazine after 0 h, 4 h, 8 h, 12 h, 16 h, 20 h and 24 h. Excitation : 497 nm.

18. Selectivity of probe 5.

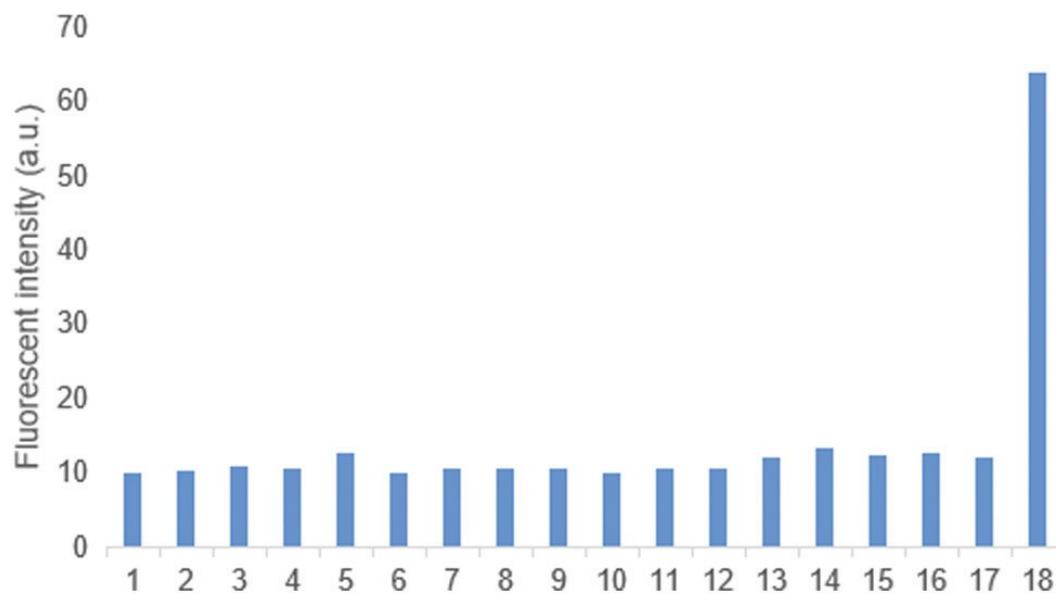
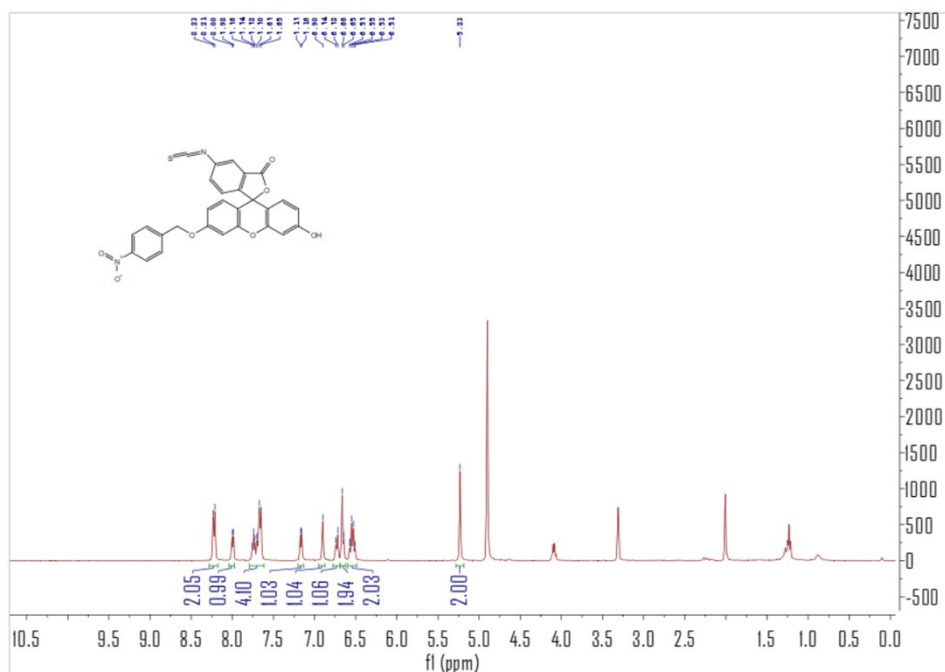


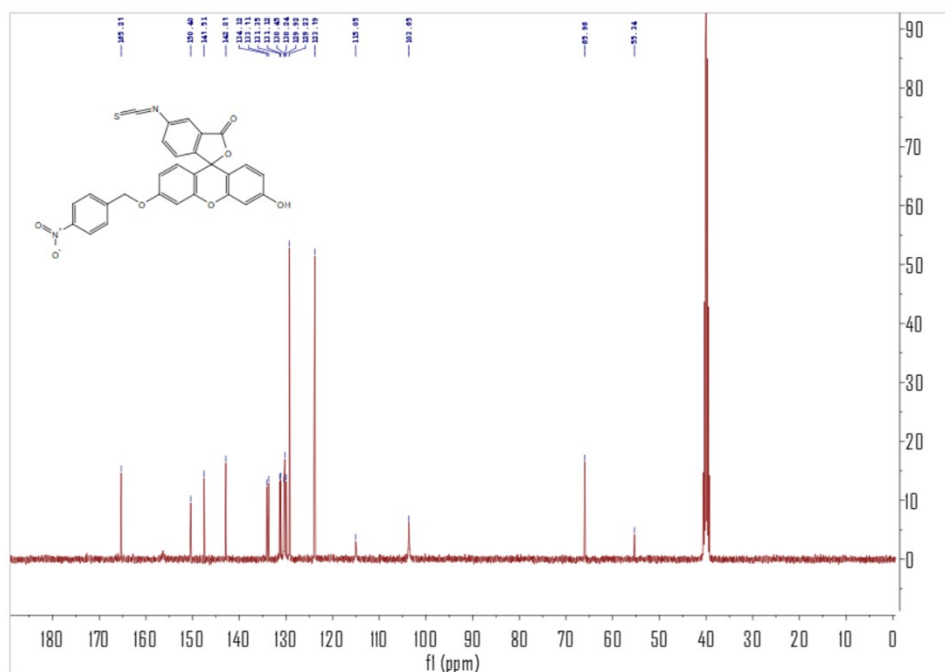
Fig. S6 Fluorescent response of probe 5 (5 μM) treated with various species. 1, blank; 2, NaCl (100 mM); 3, KCl (100 mM); 4, MgCl₂ (2.5 mM); 5, H₂O₂ (100 μM) ; 6, Tyr (1 mM); 7, His (1 mM); 8, GSH (1 mM); 9, Gly (1 mM); 10, Glu (1 mM); 11, Cys (1 mM); 12, Ala (1 mM); 13, CO (100 μM); 14, H₂S (100 μM); 15, HClO (100 μM); 16, ¹O₂ (100 μM); 17, ·OH (100 μM); 18, Formylhydrazine (100 μM).

19. ¹H NMR and ¹³C Spectra.

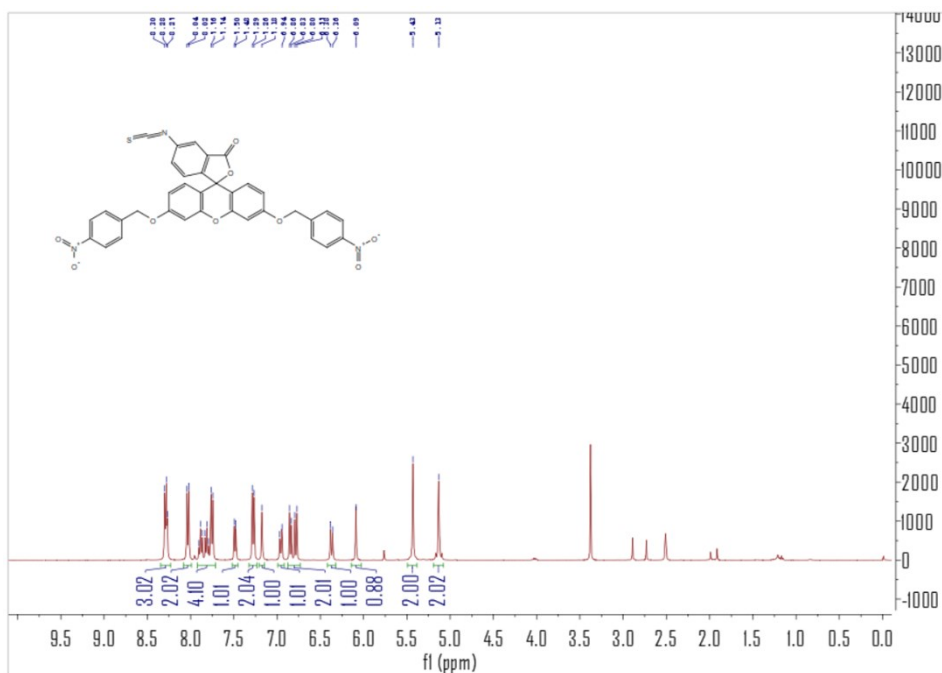
¹H NMR spectrum of 3'-hydroxy-5-isothiocyanato-6'-((4-nitrobenzyl)oxy)-3H-spiro[isobenzofuran-1,9'-xanthen]-3-one (I₁).



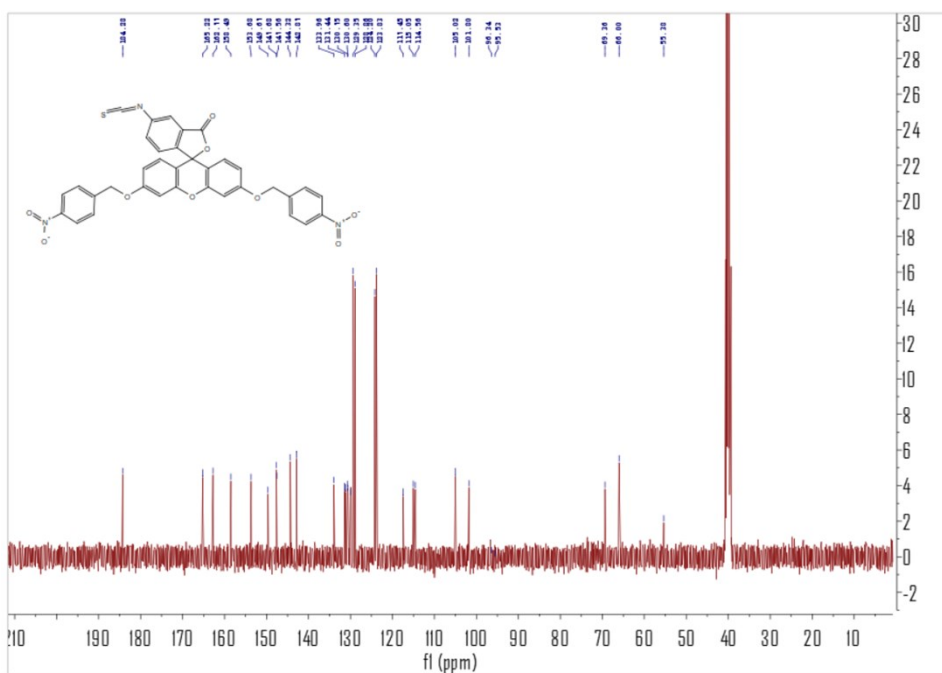
¹³C NMR spectrum of 3'-hydroxy-5-isothiocyanato-6'-((4-nitrobenzyl)oxy)-3H-spiro[isobenzofuran-1,9'-xanthen]-3-one (I₁).



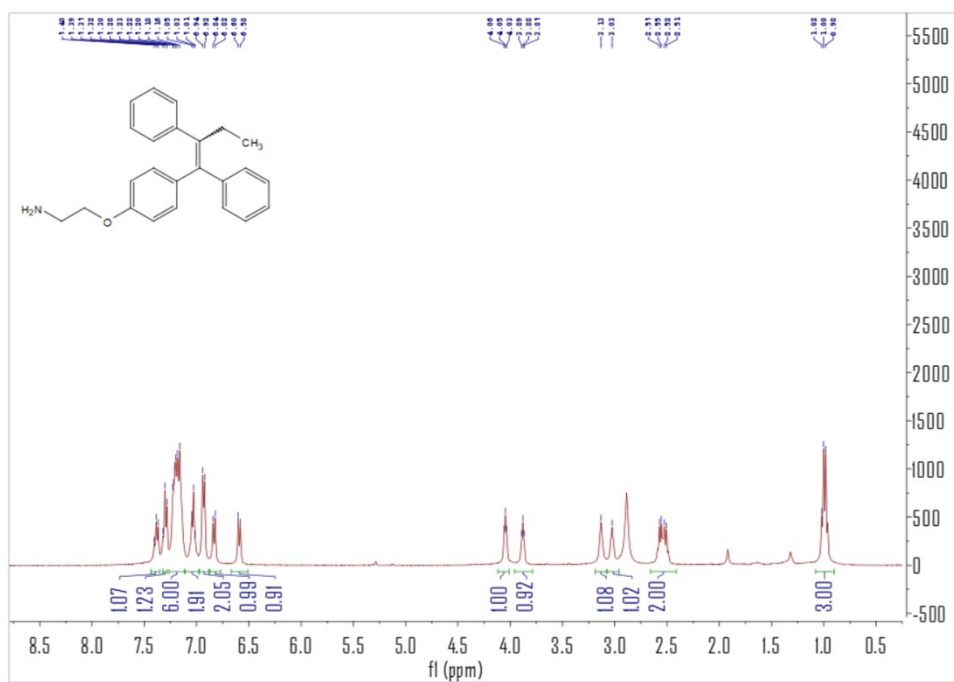
¹H NMR spectrum of 5-isothiocyanato-3',6'-bis((4-nitrobenzyl)oxy)-3H-spiro[isobenzofuran-1,9'-xanthen]-3-one (I₂).



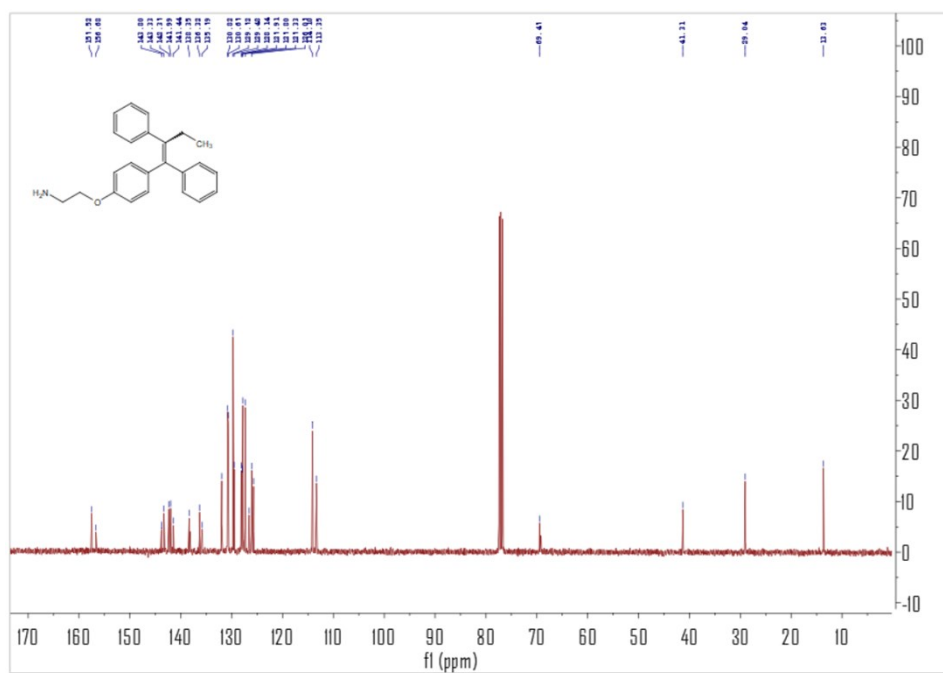
¹³C NMR spectrum of 5-isothiocyanato-3',6'-bis((4-nitrobenzyl)oxy)-3H-spiro[isobenzofuran-1,9'-xanthen]-3-one (I₂).



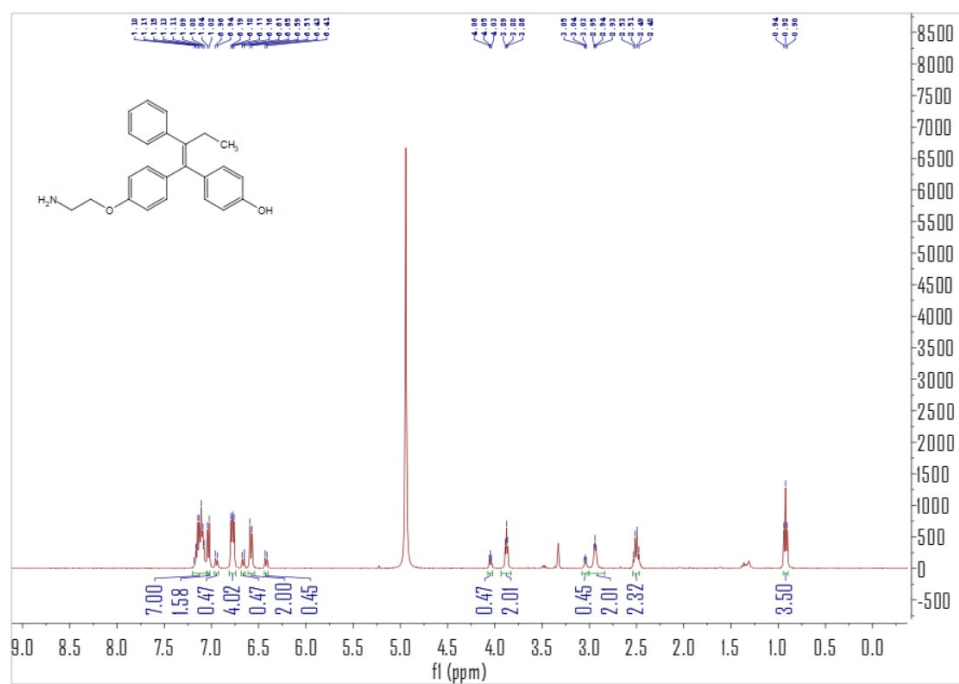
¹H NMR spectrum of (*E,Z*)-2-(4-(1,2-phenylbut-1-en-1-yl)phenoxy)ethan-1-amine (**1a**).



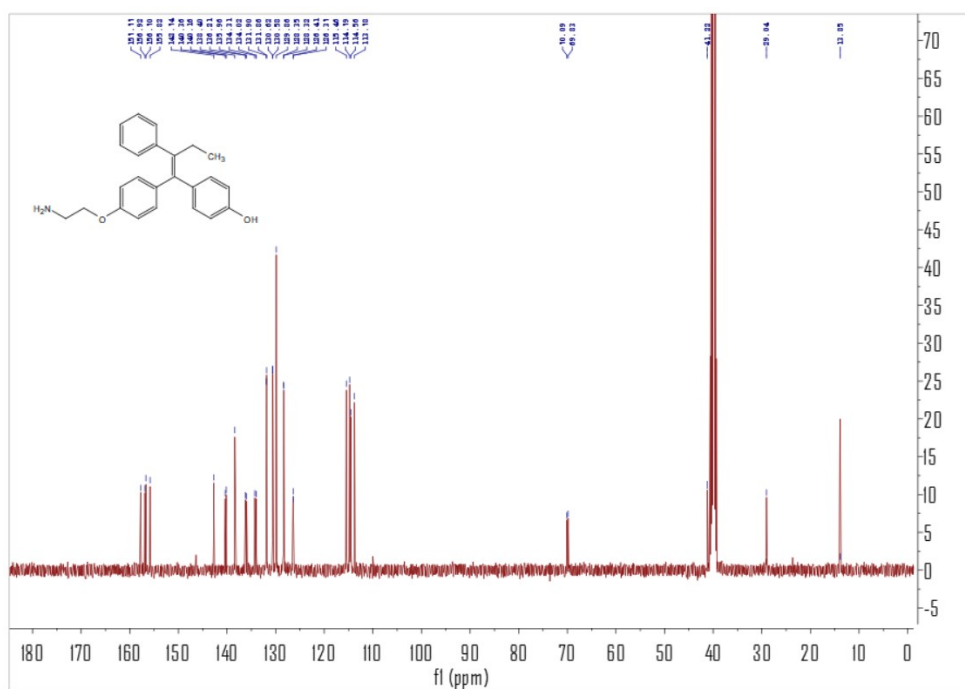
¹³C NMR spectrum of (*E,Z*)-2-(4-(1,2-phenylbut-1-en-1-yl)phenoxy)ethan-1-amine (**1a**).



¹H NMR spectrum of (Z)-4-(1-(4-(2-Aminoethoxy)phenyl)-2-phenylbut-1-enyl) phenol (I₅).



¹³C NMR spectrum of (Z)-4-(1-(4-(2-Aminoethoxy)phenyl)-2-phenylbut-1-enyl) phenol (I₅).



20. References.

1. C. Tang, Y. Du, Q. Liang, Z. Cheng, J. Tian. A Novel Estrogen Receptor α -targeted Near-Infrared Fluorescent Probe for *in Vivo* Detection of Breast Tumor. *Mol. Pharmaceutics*, 2018, **15**, 4702-4709.
2. D. Yu, B. M. Forman. Simple and Efficient Production of (Z)-4-Hydroxytamoxifen, a Potent Estrogen Receptor Modulator. *J. Org. Chem.*, 2003, **68**, 9489-9491.
3. S. Gauthier, J. Mailhot, F. Labrie. New Highly Stereoselective Synthesis of (Z)-4-Hydroxytamoxifen and (Z)-4-Hydroxytoremifene via McMurry Reaction. *J. Org. Chem.*, 1996, **61**, 3890-3893.
4. S. Zhang, Z. Wang, Z. Hu, C. Li, C. Tang, K. E. Carlson, J. Luo, C. Dong, J. A. Katzenellenbogen, J. Huang and H. B. Zhou. Selenophenes: Introducing a New Element into the Core of Non-steroidal Estrogen Receptor Ligands. *Chem. Med. Chem.*, 2017, **12**, 235-249.
5. K. W. Nettles, J. B. Bruning, G. Gil, E. E. O'Neill, J. Nowak, Y. Guo, Y. Kim, E. R. DeSombre, R. Dilis, R. N. Hanson, A. Joachimiak and G. L. Greene. Structural Plasticity in the Estrogen Receptor Ligand-Binding Domain. *EMBO Rep.*, 2007, **8**, 563-568.
6. R. E. Mewshaw, R. J. Edsall, C. J. Yang, E. S. Manas, Z. B. Xu, R. A. Henderson, J. C. Keith and H. A. Harris. ERbeta Ligands. 3. Exploiting Two Binding Orientations of the 2-phenylnaphthalene Scaffold to Achieve ERbeta Selectivity. *J. Med. Chem.*, 2005, **48**, 3953-3979.